Original paper

Rietveldite, $Fe(UO_2)(SO_4)_2(H_2O)_5$, a new uranyl sulfate mineral from Giveaway-Simplot mine (Utah, USA), Willi Agatz mine (Saxony, Germany) and Jáchymov (Czech Republic)

Anthony R. KAMPF[1*], Jiří SEJKORA[2], Thomas WITZKE[3], Jakub PLÁŠIL[4], Jiří ČEJKA[2], Barbara P. NASH[5], Joe MARTY[6]

[1] *Mineral Sciences Department, Natural History Museum of Los Angeles County, 900 Exposition Boulevard, Los Angeles, CA 90007, USA; akampf@nhm.org*
[2] *Department of Mineralogy and Petrology, National Museum, Cirkusová 1740, 193 00 Prague 9, Czech Republic*
[3] *PANalytical B.V., Lelyweg 1, 7602 EA Almelo, The Netherlands*
[4] *Institute of Physics, Academy of Sciences of the Czech Republic v.v.i, Na Slovance 2, 182 21 Prague 8, Czech Republic*
[5] *Department of Geology and Geophysics, University of Utah, Salt Lake City, Utah 84112, USA*
[6] *5199 East Silver Oak Road, Salt Lake City, UT 84108, USA*
[*] *Corresponding author*

Rietveldite (IMA2016–081), $Fe(UO_2)(SO_4)_2{\cdot}5H_2O$, is a new uranyl sulfate mineral described from three localities: Giveaway-Simplot mine (Utah, USA), Willi Agatz mine (Saxony, Germany) and Jáchymov (Western Bohemia, Czech Republic). The mineral rarely occurs in blades up to 0.5 mm long, in association with other post-mining supergene uranyl sulfates and U-free sulfates. Rietveldite is orthorhombic, space group $Pmn2_1$, a = 12.9577(9), b = 8.3183(3), c = 11.2971(5) Å, V = 1217.7(1) Å^3 and Z = 4. Thin blades are elongated on [001] and flattened on {010}. Rietveldite is brownish yellow; powdery aggregates have yellowish beige color; and it has a white streak. It does not exhibit fluorescence under either long- or short-wave UV. It is transparent to translucent with a vitreous luster. Crystals are brittle, with curved fracture and Mohs hardness ~2. Cleavage is good on {010}, and fair on {100} and {001}. Rietveldite is easily soluble in room-temperature H_2O. The density is 3.31 g/cm^3. Rietveldite is optically biaxial (+), with α = 1.570(1), β = 1.577(1) and γ = 1.586(1) (white light); $2V_{calc.}$ = 83.3°, $2V_{meas.}$ = 82(1)°. Dispersion is very strong ($r > v$). Rietveldite exhibits barely noticeable pleochroism in shades of light brownish yellow color, $Y < X \approx Z$. The optical orientation is X = **b**, Y = **a**, Z = **c**. Chemical analyses for rietveldite from Giveaway-Simplot (WDS, 4 spots on 2 crystals) provided FeO 9.56, ZnO 1.06, MgO 0.14, MnO 0.10, SO_3 26.99, UO_3 47.32, H_2O (calc.) 15.39, total 100.56 wt. %, which yields the empirical formula $(Fe_{0.79}Zn_{0.08}Mg_{0.02}Mn_{0.01})_{\Sigma 0.90}(UO_2)_{0.99}(SO_4)_{2.01}{\cdot}5.10H_2O$ (based on 15 O *apfu*). Prominent features in the Raman and infrared spectra include the O–H stretching vibrations, symmetric and antisymmetric stretching vibrations of $(UO_2)^{2+}$ ion, and stretching and bending vibrations of symmetrically non-equivalent $(SO_4)^{2-}$ groups. The eight strongest powder X-ray diffraction lines are [d_{obs} Å ($I_{rel.}$) (*hkl*)]: 8.309(34)(010), 6.477(100)(200), 5.110(58)(210), 4.668(48)(012), 4.653(36)(211), 3.428(41)(013), 3.341(33)(221), 3.238(49)(400). The crystal structure of rietveldite (R_1 = 0.037 for 2396 reflections with $I_{obs} > 2\sigma[I]$) contains infinite uranyl sulfate chains of composition $[(UO_2)(SO_4)_2(H_2O)]^{2-}$ along [001]. The adjacent chains are linked in the [100] direction by FeO_6 octahedra, which share vertices with SO_4 tetrahedra resulting in a heteropolyhedral sheet parallel to {010}; adjacent sheets are linked by hydrogen bonding only. The uranyl sulfate chains are the same as those in the structures of several other uranyl sulfate minerals. Rietveldite is named for Hugo M. Rietveld (1932–2016).

Keywords: rietveldite, new mineral, uranyl sulfate, crystal structure, polytype, bond-valence
Received: 29 December, 2016; accepted: 24 April, 2017; handling editor: F. Laufek
The online version of this article (doi: 10.3190/jgeosci.236) contains supplementary electronic material.

1. Introduction

Uranyl sulfates are common supergene alteration products formed by oxidation–hydration weathering of uraninite (Plášil 2014) associated with sulfides, such as pyrite or chalcopyrite (Finch and Murakami 1999; Krivovichev and Plášil 2013). More specifically, in old mining workings, oxidizing weathering of sulfides generates low-pH solutions that react with coliform uraninite, also known as *pitchblende*, to form the uranyl sulfates (Fernandes et al. 1995; Brugger et al. 2003; Plášil et al. 2014).

Rietveldite is a new uranyl sulfate mineral found at three localities: the Giveaway-Simplot mine in Utah (USA), the Willi Agatz mine in Saxony (Germany), and Jáchymov (Joachimsthal), Czech Republic. The new mineral and the name were approved by the Commission on New Minerals, Nomenclature and Classification of the International Mineralogical Association (IMA2016–081).

The new mineral, rietveldite (/'ri:t veld ait/), is named in honor of prominent Dutch crystallographer Hugo M. Rietveld (1932–2016). For much of his scientific career, Hugo Rietveld was involved in the study of uranium compounds (Rietveld 1966; Loopstra and Rietveld 1969). In 1967, he developed a program for the refinement of neutron diffraction data (Rietveld 1967, 1969). The refinement approach, now well-known as *the Rietveld method*, was further developed for the refinement of crystal structures from powder X-ray diffraction data and for the quantitative phase analysis (Young 1993).

The mineral description is based on four cotype specimens. Two cotypes from the Giveaway-Simplot mine are deposited in the collections of the Natural History Museum of Los Angeles County, 900 Exposition Boulevard, Los Angeles, CA 90007, USA, catalogue numbers 66291 and 66292. One cotype from the Willi Agatz mine is deposited in the collections of the TU Bergakademie Freiberg, Akademiestrasse 6, Freiberg, 09599, Germany, catalogue number 84140. The last cotype from Jáchymov is deposited in the collections of the Department of Mineralogy and Petrology, National Museum, Cirkusová 1740, 193 00 Prague 9, Czech Republic, catalogue number P1N 45564.

2. Occurrence

2.1. Giveaway-Simplot mine (Utah, USA)

The mineral was found on specimens collected underground in the Giveaway-Simplot mine (37.552500 N 110.282778 W), in the White Canyon mining district, San Juan County, Utah, USA. The Giveaway-Simplot mine is located on the east side of Red Canyon. The geology of this deposit is similar to that of the Blue Lizard, some 1.4 km to the NE (Chenoweth 1993; Kampf et al. 2015c). Mineralized channels occur in the Shinarump Member of the Chinle Fm. The Shinarump Member consists of medium- to coarse-grained sandstone or conglomeratic sandstone beds and thick siltstone lenses. Ore minerals were deposited as replacements of wood and other organic material and as disseminations in the enclosing sandstone. Since the mine closed, oxidation of primary ores in the humid underground environment has produced a variety of secondary minerals, mainly sulfates, as efflorescent crusts on the surfaces of mine walls. Rietveldite is a rare mineral in the secondary uranyl sulfate mineral assemblages. It has been found on asphaltum in association with ferricopiapite, gypsum, römerite and shumwayite (Kampf et al. 2017) and on pyrite-impregnated sandstone in association with gypsum, halotrichite and römerite.

2.2. Willi Agatz mine (Saxony, Germany)

Small crystals of rietveldite occur very sparsely on the +50 m level, Willi Agatz mine, Gittersee mining field, Dresden, Sachsen (Saxony), Germany (51.004941 N, 13.693927 E) as a weathering product of uranium-bearing coal and pyrite. Mining of Upper Carboniferous coal for energy production started in 1950. During the periods 1952–1955 and 1968–1989, the coal was mined for the production of uranium. The mine was closed in 1990. Sedimentary rocks in the coal basin include, among others, shales, siltstones, sandstones, conglomerates, and pyroclastics. The U content in the coal and carbon-rich shale differs locally and according to the coal type; average values range from 0.1 to 0.5 %, with a maximum of 1 % U_3O_8 (Thalheim et al. 1991; Reichel and Schauer 2006). Rietveldite at the Willi Agatz mine is associated with halotrichite, krausite, melanterite, native sulfur and voltaite.

Fig. 1 Rietveldite on asphaltum from the Giveaway-Simplot mine; width of photograph 1.7 mm.

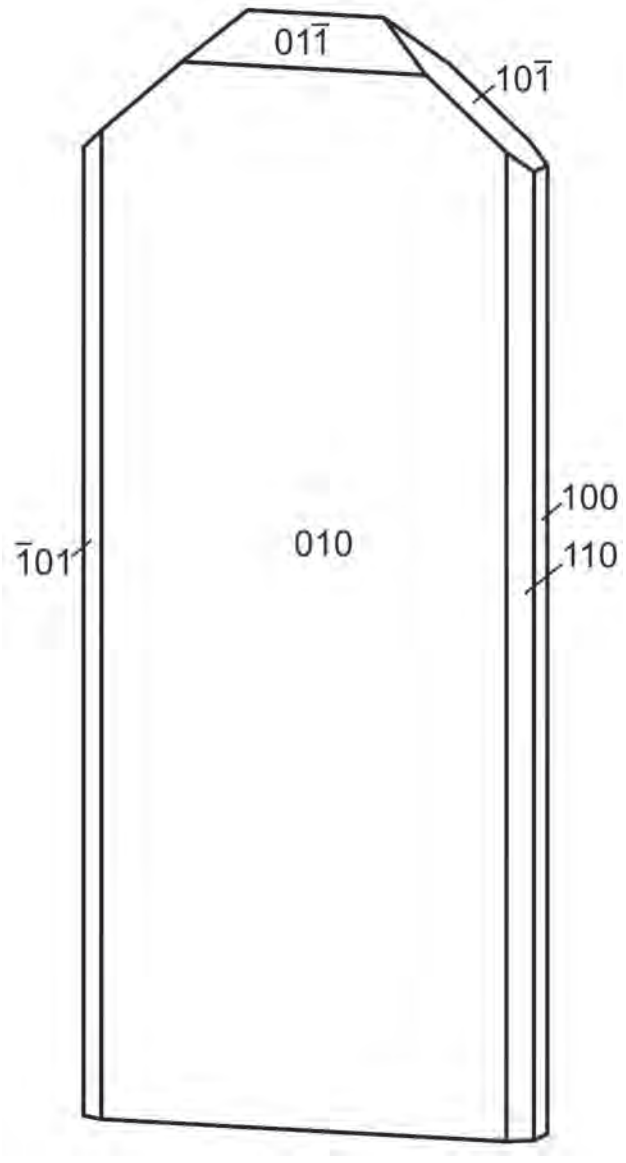

Fig. 2 Crystal drawing of rietveldite from the Giveaway-Simplot mine; clinographic projection.

2.3. Jáchymov (Western Bohemia, Czech Republic)

Rietveldite was identified on one historical museum sample from the Jáchymov ore district, Western Bohemia, Czech Republic. The Jáchymov ore district is a classic example of an Ag–As–Bi–Co–Ni–U hydrothermal vein type deposit (Ondruš et al. 2003). The ore-bearing veins cut medium-grade metasedimentary rocks of Cambrian to Ordovician age, intruded by a Variscan granitic pluton. The majority of the primary ore minerals were deposited from mesothermal fluids associated with Variscan mineralizing processes. About 450 minerals have been described from this ore district to date, including an extremely diverse assemblage of supergene minerals

Fig. 3 Rietveldite crystals from the Willi Agatz mine; SE image by B. Ullrich (TU Bergakademie Freiberg).

(Hloušek et al. 2014), among which are fifty for which Jáchymov is the type locality. Rietveldite occurs in strongly altered gangue in association with rozenite, shumwayite (Kampf et al. 2017) and an as yet unnamed Al–uranyl sulfate.

3. Physical and optical properties

Rietveldite crystals from the Giveaway-Simplot mine are thin blades. Those found growing on asphalt are up to 0.5 mm long and are grouped in subparallel to random intergrowths. Those found on pyrite-impregnated sandstone are much smaller, to 0.1 mm, and form sprays (Fig. 1). Thin blades are elongated on [001] and flattened on {010} (Fig. 2). Crystals from the Willi Agatz mine are acicular to ruler-shaped blades up to 0.5 mm in length (Fig. 3), usually growing in radiating aggregates and intimately intergrown with halotrichite (Fig. 4). Rietveldite from Jáchymov occurs as microcrystalline (powdery) ag-

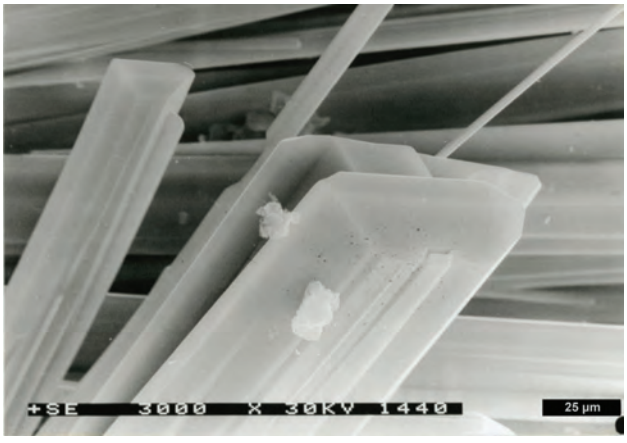

Fig. 4 Rietveldite crystals from the Willi Agatz mine; SE image by B. Ullrich (TU Bergakademie Freiberg).

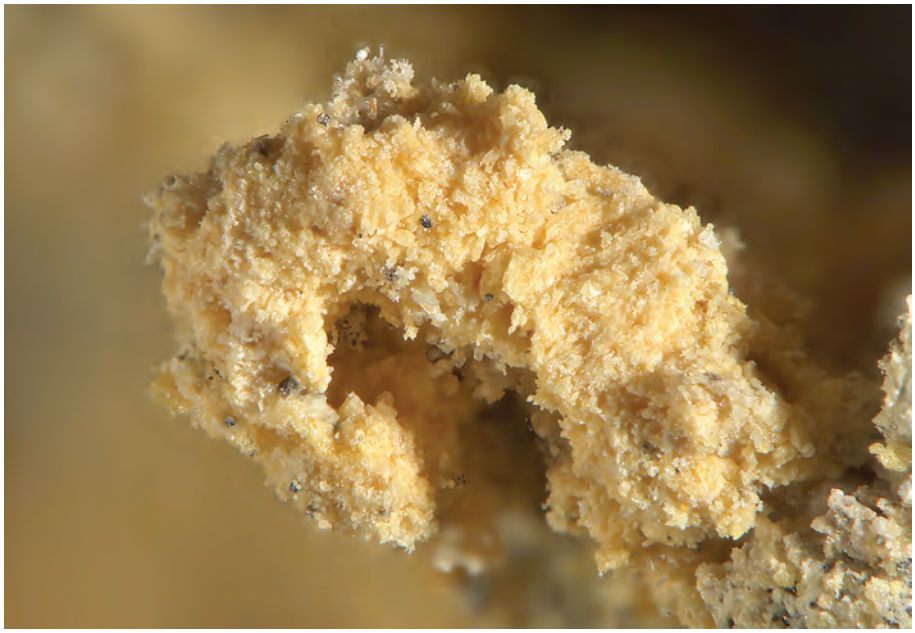

Fig. 5 Group of rietveldite crystals from Jáchymov, Czech Republic, width of photograph 1.8 mm.

gregates (Fig. 5) up to several millimeters across consisting of irregular prismatic crystals up to 60 μm (Fig. 6).

The color of individual crystals is brownish yellow; powdery aggregates have yellowish-beige color. The mineral has a white streak. Crystals are transparent (individual crystals) to translucent (in aggregates) with a vitreous luster. They are brittle, with a good cleavage on {010}, fair cleavages on {100} and {001}, and curved fracture. Rietveldite is easily soluble in room-temperature H_2O. The Mohs hardness is estimated at 2. The calculated density is 3.274 g/cm^3 based on the unit-cell dimensions from single-crystal X-ray data and on the empirical formula from electron-microprobe analyses; the measured density 3.31 g/cm^3 was obtained by floatation in methylene iodide (for material from Giveaway-Simplot mine). Rietveldite does not show fluorescence under either long- or short-wave ultraviolet radiation. The mineral from the Giveaway-Simplot mine is optically biaxial positive, with $\alpha = 1.570(1)$, $\beta = 1.577(1)$ and $\gamma = 1.586(1)$ (measured in white light), $2V_{meas.} = 82(1)°$, $2V_{calc.} = 83.3°$. Dispersion is very strong ($r > v$). Rietveldite crystals are light brownish yellow in plane-polarized light and exhibit barely noticeable pleochroism, $Y < X \approx Z$. The optical orientation is X = **b**, Y = **a**, Z = **c**. The Gladstone-Dale compatibility, $1 - (K_p/K_c)$, is superior (–0.008) for the empirical formula and using the $k(UO_3) = 0.118$ (Mandarino 1976).

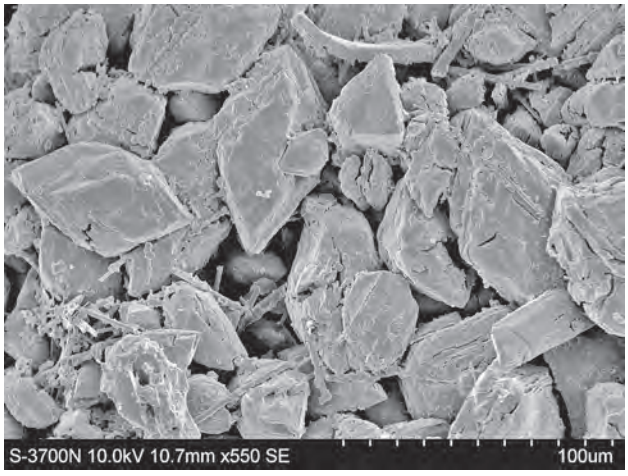

Fig. 6 Irregular rietveldite crystals from Jáchymov, Czech Republic, SE image.

4. Thermal analysis of rietveldite

Thermal analysis (thermal-gravimetry, TG) of rietveldite from Jáchymov was carried out by means of a Stanton-Redcroft TG-750 thermobalance (Fig. 7); sample weight 2.343 mg, heating rate 10 °C/min and air flow 20 ml/min (Institute of Chemical Technology in Prague, Czech Republic). Rietveldite dehydrates in two steps: at 20–150 °C 4.70 wt. % (~1.5 H_2O) and 150–320 °C 10.05 wt. % (~3.5 H_2O). At 320–900 °C, $FeSO_4$ and β-UO_2SO_4 form; however, a small amount of SO_3 may be released. Thermal decomposition of anhydrous $FeSO_4$ and UO_2SO_4 may also partly overlap (509–900 °C). It is related to the solid-state formation of FeU_3O_{10} and Fe_2O_3 and release of SO_3 and O_2, and by decomposition of FeU_3O_{10}. Both U_3O_8 and Fe_2O_3 are expected to be end-products of the thermal decomposition of rietveldite; however, from the character of the TG curve, it may be inferred that thermal decomposition is not finished at 900 °C and continues at higher temperatures.

Because insufficient material from the Giveaway-Simplot mine was available for a direct determination

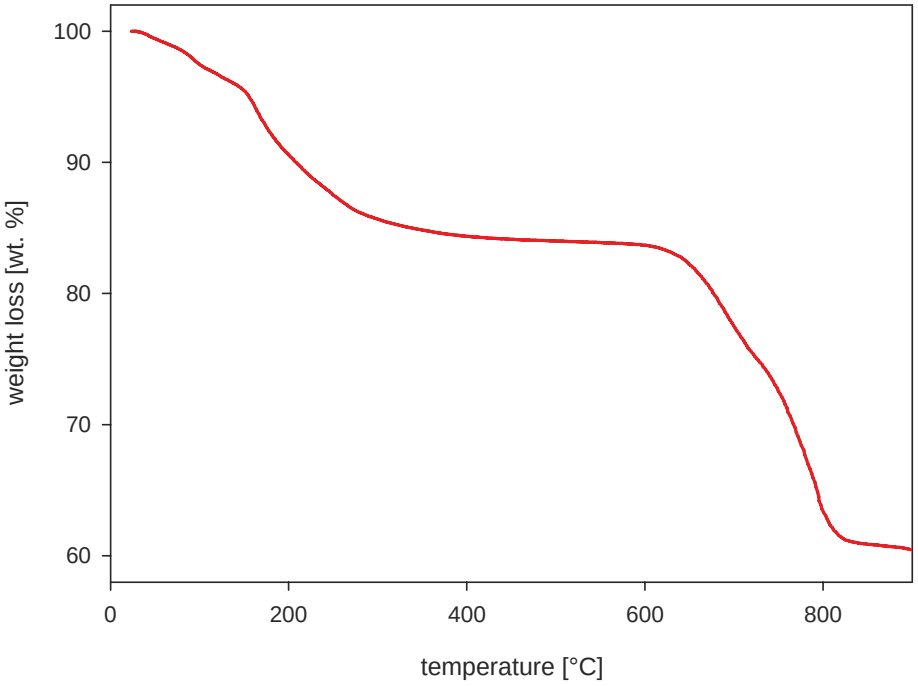

Fig. 7 Thermal-gravimetric curve of rietveldite from Jáchymov.

of H_2O, it has been calculated based upon the structure determination; however, it is noteworthy that the calculated H_2O is between the experimental TG values for material from Jáchymov and the Willi Agatz mine (Tab. 2).

5. Chemical composition

The chemical composition of rietveldite was determined using different analytical facilities for materials from the three individual localities.

Material from the Giveaway-Simplot mine (Tab. 1) was analyzed using a Cameca SX-50 electron microprobe (University of Utah) with four wavelength dispersive spectrometers and using Probe for EPMA software (Probe Software, Inc.). Analytical conditions were 15 kV accelerating voltage, 10 nA beam current and a beam diameter of 5 μm. Counting times were 20 s on both peak and background for each element. Raw X-ray intensities were corrected for matrix effects with a φρ(Z) algorithm (Pouchou and Pichoir 1985).

Chemistry of rietveldite from Willi Agatz mine was determined by means of an electron microprobe (Camebax, WDX mode, 10 kV, 10 nA).

The chemical composition of rietveldite from Jáchymov was determined using a Cameca SX-100 electron microprobe (Faculty of Science, Masaryk University, Brno) with five wavelength dispersive spectrometers. Analytical conditions were: 15 kV accelerating voltage, 2 nA beam current and a beam diameter of 2 μm. Counting times were 20 s both on peak and background for each element. Raw X-ray intensities were corrected for matrix effects with a φρ(Z) algorithm (Pouchou and Pichoir 1985).

The empirical formula for rietveldite from the Giveaway-Simplot mine is $(Fe_{0.79}Zn_{0.08}Mg_{0.02}Mn_{0.01})_{\Sigma 0.90}(UO_2)_{0.99}(SO_4)_{2.01}\cdot 5.10H_2O$ (calculated on the basis of 15 O apfu + 0.24 H for charge balance).

The empirical formula of rietveldite from the Willi Agatz mine is $(Fe_{0.76}Mn_{0.20}Mg_{0.07})_{\Sigma 1.03}(UO_2)_{0.98}(SO_4)_{1.91}\cdot 5.29H_2O$.

The empirical formula of rietveldite from Jáchymov is $(Fe_{0.88}Zn_{0.05}Mn_{0.03}Mg_{0.01})_{\Sigma 0.97}(UO_2)_{1.01}(SO_4)_{2.01}\cdot 4.98H_2O$ (calculated on the basis of 15 O apfu).

The ideal formula of rietveldite, $Fe(UO_2)(SO_4)_2\cdot 5H_2O$, requires FeO 11.82, UO_3 47.04, SO_3 26.33 and H_2O 14.81, total 100 wt. %.

Tab. 1 Results of chemical analyses (in wt. %) of rietveldite from the Giveaway-Simplot mine

Constituent	Mean (4 points)	Range	Stand. Dev.	Probe Standard
FeO	9.56	9.31–9.91	0.29	hematite
ZnO	1.06	0.56–1.48	0.38	Zn metal
MgO	0.14	0.10–0.18	0.04	diopside
MnO	0.10	0.04–0.16	0.06	rhodonite
UO_3	47.32	46.85–47.66	0.37	syn. UO_2
SO_3	26.99	26.70–27.19	0.22	celestine
H_2O*	15.39			
Total	100.56			

* Based upon the structure

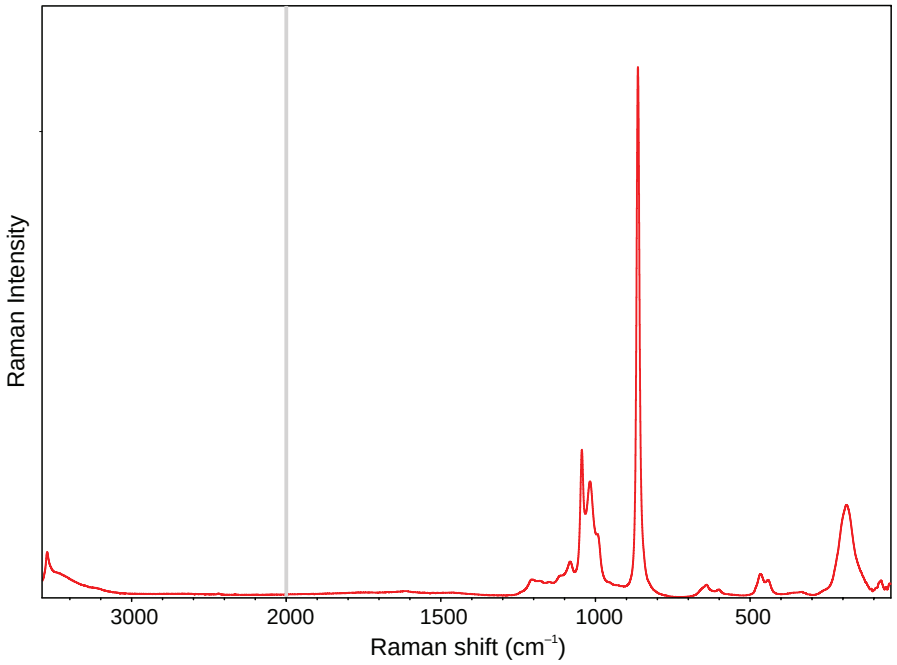

Fig. 8 Raman spectrum of rietveldite from Jáchymov.

Tab. 2 Results of chemical analyses (in wt. %) of rietveldite from Jáchymov and the Willi Agatz mine

Constituent	Jáchymov				Willi Agatz mine			
	Mean (7 points)	Range	Stand. Dev.	Probe Standard	Mean (6 points)	Range	Stand. Dev.	Probe Standard
FeO	10.34	10.07–10.83	0.29	almandine	9.02	8.57–9.60	0.40	pyrite
ZnO	0.61	0.36–0.86	0.19	gahnite				
MgO	0.06	0.00–0.15	0.06	syn. Mg_2SiO_4	0.48	0.45–0.51	0.02	spinel
MnO	0.36	0.22–0.52	0.10	spessartine	2.32	1.96–2.99	0.36	Mn metal
UO_3	47.39	46.50–48.87	0.82	uranophane	46.62	45.56–48.30	0.95	syn. U_3O_8
SO_3	26.46	25.61–28.74	0.98	syn. $SrSO_4$	25.39	24.88–25.98	0.38	pyrite
H_2O	14.75*				15.80*			
Total	99.97				99.63			

* From thermal analysis

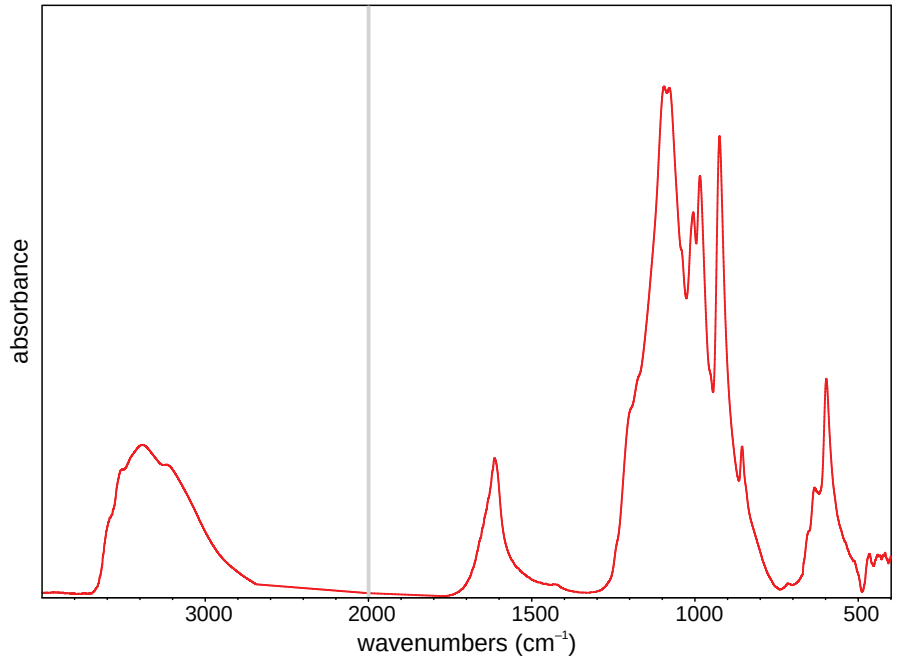

Fig. 9 Infrared spectrum of rietveldite from Jáchymov.

6. Vibration spectroscopy

6.1. Raman spectroscopy

The Raman spectrum of rietveldite (Jáchymov sample) was collected in the range 3580–45 cm^{-1} using a DXR dispersive Raman spectrometer (Thermo Scientific) mounted on a confocal Olympus microscope (Fig. 8). The Raman signal was excited by a green 532 nm diode-pumped solid-state laser and detected by a CCD detector. The experimental parameters were: 10× objective, 1 s exposure time, 1000 exposures, 900 lines/mm grating, 50 μm pinhole spectrograph aperture and 4 mW laser power level (limited to avoid possible thermal destruction of sample). The instrument was set up by a software-controlled calibration procedure using multiple neon emission lines (wavelength calibration), multiple polystyrene Raman bands (laser frequency calibration) and standardized white-light sources (intensity calibration). Spectral manipulations were performed using the Omnic 9 software (Thermo Scientific).

The general features of the vibration spectra of uranyl sulfate minerals and their characteristics were thoroughly reviewed by Čejka (1999). In the structure of orthorhombic rietveldite, space group $Pmn2_1 - C^7_{2v}$, $Z = 4$, there are present one symmetrically distinct U^{6+}, two symmetrically distinct Fe^{2+}, and two symmetrically distinct S^{6+}. According to Serezhkina et al. (1979), observed numbers of IR/RA bands are lower than expected from site and factor group analyses. This may be caused by overlapping of corresponding bands and/or limited resolution power of the instrument used. Observed Raman and infrared bands are comparable and in agreement with those of synthetic $M^{2+}(UO_2)(SO_4)_2 \cdot 5H_2O$ (Serezhkina et al. 1979; Serezhkin and Serezhkina 1982).

The main bands observed are (wavenumbers, in cm^{-1}): 3543, 3476, 1616, 1206, 1181, 1110, 1083, 1044, 1018, 991, 862, 659, 641, 602, 466, 441, 365, 336, 266, 249, 234, 222, 206, 186, 148, 133, 107, 94 and 78 cm^{-1}. Raman bands at 3543 and 3476 cm^{-1} are assigned to the ν O–H stretching vibrations of hydrogen bonded structurally non-equivalent H_2O molecules. According to Libowitzky (1999), approximate O–H···O hydrogen bond lengths 2.98 and 2.87 Å were inferred from these wavenumbers, respectively. A weak Raman band at 1616 cm^{-1} is assigned to the ν_2 (δ) bending vibrations of H_2O molecules. Lowering of the T_d symmetry of free $(SO_4)^{2-}$ ion may cause splitting of degenerate vibrations and activation of all vibrations in infrared and Raman spectra. Raman bands at 1206, 1181, 1110, 1083

Tab. 3 Powder diffraction data for rietveldite

$I_{obs.}$	$d_{obs.}$	$d_{calc.}$	$I_{calc.}$	*h*	*k*	*l*	$I_{obs.}$	$d_{obs.}$	$d_{calc.}$	I_{calc}	*h*	*k*	*l*
34	**8.309**	8.310	43	0	1	0	2	2.0695	2.0695	14	4	3	1
20	6.691	6.693	28	0	1	1	8	2.0664	2.0655	8	2	1	5
100	**6.477**	6.478	100	2	0	0	3	2.0616	2.0615	8	4	1	4
12	5.645	5.646	16	0	0	2	6	2.0550	2.0550	10	6	1	1
58	**5.110**	5.109	70	2	1	0	5	2.0168	2.0168	9	6	0	2
48	**4.668**	4.670	45	0	1	2	6	1.9841	1.9842	10	0	2	5
36	**4.653**	4.655	54	2	1	1	8	1.9774	1.9771	4	0	3	4
28	4.255	4.256	38	2	0	2	3	1.9598	1.9599	6	6	1	2
6	4.154	4.155	7	0	2	0	6	1.9494	1.9497	8	0	4	2
5	4.037	4.034	2	3	0	1	5	1.8972	1.8972	11	2	2	5
26	3.899	3.899	53	0	2	1	4	1.8895	1.8890	9	6	2	1
23	3.788	3.788	33	2	1	2	5	1.8819	1.8819	10	0	0	6
1	3.627	3.629	1	3	1	1	10	1.8670	1.8669	21	2	4	2
1	3.496	3.497	1	2	2	0	2	1.8367	1.8373	4	4	3	3
41	**3.428**	3.429	51	0	1	3	2	1.8269	1.8271	4	6	1	3
33	**3.341**	3.341	42	2	2	1	1	1.8186	1.8188	2	0	4	3
49	**3.238**	3.239	38	4	0	0	3	1.8072	1.8072	5	2	0	6
26	3.029	3.030	38	2	1	3	3	1.7660	1.7659	7	2	1	6
5	3.018	3.018	6	4	1	0	4	1.7502	1.7503	7	0	3	5
11	2.972	2.973	13	2	2	2	3	1.7148	1.7151	7	6	0	4
9	2.915	2.915	11	4	1	1	5	1.7074	1.7075	12	6	2	3
5	2.822	2.823	7	0	0	4	5	1.6901	1.6897	11	2	3	5
4	2.810	2.809	6	4	0	2	3	1.6842	1.6839	6	6	3	1
13	2.789	2.789	13	0	2	3	3	1.6706	1.6704	8	4	4	2
16	2.690	2.690	18	0	3	1	3	1.6273	1.6272	8	4	0	6
9	2.673	2.673	12	0	1	4	5	1.6198	1.6200	6	2	4	4
7	2.661	2.661	11	4	1	2	3	1.5942	1.5943	3	0	5	2
10	2.588	2.588	15	2	0	4			1.5937	2	2	5	1
13	2.562	2.562	22	2	2	3	1	1.5839	1.5835	2	0	1	7
9	2.547	2.547	12	2	3	0	1	1.5741	1.5740	3	8	1	1
9	2.4912	2.4915	15	4	2	1	1	1.5568	1.5567	3	8	0	2
14	2.4851	2.4845	14	2	3	1	2	1.5481	1.5481	6	2	5	2
5	2.4707	2.4708	6	2	1	4	3	1.5394	1.5399	6	4	3	5
7	2.3543	2.3545	14	4	1	3	2	1.5299	1.5301	4	8	1	2
2	2.3263	2.3273	2	4	2	2	1	1.5138	1.5136	4	2	3	6
1	2.3217	2.3216	3	2	3	2	1	1.5038	1.5037	3	0	2	7
7	2.2308	2.2309	8	0	3	3	2	1.4956	1.4956	7	8	2	1
1	2.1790	2.1793	2	0	1	5	2	1.4868	1.4866	3	4	4	4
1	2.1595	2.1593	1	6	0	0	1	1.4788	1.4787	3	4	5	0
3	2.1281	2.1281	7	4	0	4	3	1.4647	1.4648	5	2	2	7
6	2.1136	2.1137	15	4	2	3			1.4643	4	8	1	3
8	2.1093	2.1093	11	2	3	3	1	1.4609	1.4610	4	6	2	5
5	2.0897	2.0899	9	6	1	0	2	1.4471	1.4471	7	6	4	2
4	2.0774	2.0775	4	0	4	0							

d values quoted in Å;
$I_{calc.}$ calculated (Yvon et al. 1977) from the crystal structure data of rietveldite (Tabs 5 and 6)

Tab. 4 Refined unit cell parameters for rietveldite

Occurrence	*a*	*b*	*c*	*V*
Giveaway-Simplot mine[1]	12.9577(9)	8.3183(3)	11.2971(5)	1217.7(1)
Giveaway-Simplot mine[2]	12.930(1)	8.3052(6)	11.2819(8)	1211.5(2)
Jáchymov[3]	12.9557(5)	8.3098(3)	11.2915(4)	1215.64(6)
Willi Agatz mine[4]	12.952(6)	8.301(3)	11.224(5)	1206.7(9)

[1] Single-crystal data (for conditions see text)
[2] Powder data obtained using a Rigaku R-Axis Rapid II curved imaging plate microdiffractometer with monochromatized MoK_α radiation; a Gandolfi-like motion on the ϕ and ω axes was used to randomize the sample; observed *d* spacings and intensities were derived by profile fitting using JADE 2010 software (Materials Data, Inc.); unit cell parameters were refined from the powder data using a whole-pattern fitting Rietveld analysis in JADE 2010
[3] Powder data (for conditions see text)
[4] Single-crystal data obtained Rigaku/Oxford Diffraction SuperNova diffractometer with Atlas S2 CCD detector and using MoK_α radiation from the microfocus source

and 1044 cm^{-1} are attributed to the triply degenerate ν_3 $(SO_4)^{2-}$ antisymmetric stretching vibrations, and Raman bands at 1018 and 991 cm^{-1} to the ν_1 $(SO_4)^{2-}$ symmetric stretching vibrations. The band with the highest Raman intensity at 862 cm^{-1} corresponds to the ν_1 $(UO_2)^{2+}$ symmetric stretching vibration; no band was observed

Tab. 5 Crystallographic data and refinement details for rietveldite from the Giveaway-Simplot mine

Crystal data	
Formula	$(Fe_{0.82}Zn_{0.18})(UO_2)(SO_4)_2(H_2O)_5$
Crystal system	orthorhombic
Space group	$Pmn2_1$
Unit-cell parameters: *a*, *b*, *c* [Å]	12.9577(9), 8.3183(3), 11.2971(5)
Unit-cell volume [Å^3]	1217.67(11)
Z	4
Calculated density [g/cm^3]	3.326
Crystal size [mm]	0.180 × 0.090 × 0.005
Data collection	
Diffractometer	Rigaku R-Axis Rapid II
Temperature [K]	293
Radiation, wavelength [Å]/power	MoK_α (λ = 0.71075 Å) / 50 kV, 40 mA
θ range for data collection [º]	3.14–30.02
Limiting Miller indices	h = –18→18, k = –9→11, l = –12 → 15
Total reflections collected	7555
Unique reflections	2885
Unique observed reflections, criterion	2396 [$I > 2\sigma(I)$]
Absorption coefficient [mm^{-1}], type	15.033; Abscor
R_{int}	0.056
F_{000}	1122.8
Refinement method	Shelxl, full-matrix least-squares on F^2
Parameters, restraints	188, 1
R_1, wR_2 (obs)	0.0369, 0.0788
R_1, wR_2 (all)	0.0460, 0.0846
Goodness of fit	1.057
Weighting scheme, weights	σ, w =1/(σ^2(I)+0.0004I^2)
Largest diff. peak and hole (e$^-$/Å^3)	3.56,–1.27
Absolute structure parameter	–0.003(10)
Twin matrix	$\begin{pmatrix} -1 & 0 & 0 \\ 0 & -1 & 0 \\ 0 & 0 & -1 \end{pmatrix}$

$R_{int} = \Sigma|F_o^2-F_o^2(\text{mean})|/\Sigma[F_o^2]$. GoF = $S = \{\Sigma[w(F_o^2-F_c^2)^2]/(n-p)\}^{1/2}$. $R_1 = \Sigma||F_o|-|F_c||/\Sigma|F_o|$. $wR_2 = \{\Sigma[w(F_o^2-F_c^2)^2]/\Sigma[w(F_o^2)^2]\}^{1/2}$; $w = 1/[\sigma^2(F_o^2)+(aP)^2+bP]$ where a is 0.0234, b is 0 and P is $[2F_c^2+\text{Max}(F_o^2,0)]/3$.

in the Raman spectrum of rietveldite attributable to the ν_3 $(UO_2)^{2+}$. From this wavenumber, approximate U–O bond length in uranyl 1.75 Å was inferred (Bartlett and Cooney 1989). Raman bands at 659, 641 and 602 cm^{-1} are attributed to the triply degenerate ν_4 (δ) $(SO_4)^{2-}$ bending vibrations and those at 466 and 441 cm^{-1} to the ν_2 (δ) $(SO_4)^{2-}$ doubly degenerate bending vibrations. Raman bands at 365 and 336 cm^{-1} are related to the ν (U–O_{ligand}) stretching vibrations. Raman bands in the region from 222 to 266 cm^{-1} are attributed to the doubly degenerate ν_2 (δ) $(UO_2)^{2+}$ bending vibrations. Raman bands at 206, 186, 148, 133, 107, 94 and 78 cm^{-1} can be assigned to lattice modes.

6.2. Infrared spectroscopy

The infrared vibrational spectrum of rietveldite (Jáchymov sample) was collected in the range 4000–400 cm^{-1} using Fourier-transform infrared spectrometer Nicolet iS50 on built-in attenuated total reflectance accessory with monolithic diamond crystal (Thermo Scientific), DTGS special detector. Spectral manipulations were performed using the Omnic 9 software (Thermo Scientific). The main bands (Fig. 9) observed are (wavenumbers, in cm^{-1}): 3587, 3516, 3284 3228, 1616, 1200, 1176, 1095, 1078, 1041, 1007, 985, 924, 855, 708, 655, 633, 598, 512 and 466 cm^{-1}. Infrared bands and shoulders observed at 3587, 3516, 3284 and 3228 cm^{-1} are assigned to the ν O–H stretching vibrations of hydrogen bonded structurally non-equivalent H_2O molecules. Approximate O–H···O hydrogen bond lengths vary in the range from >3.2 to 2.72 Å (Libowitzky 1999). A band at 1616 cm^{-1} is assigned to the ν_2 (δ) bending vibrations of H_2O molecules. Bands at 1200(sh), 1176(sh), 1095, 1078 and 1041(sh) are attributed to the triply degenerate ν_3 $(SO_4)^{2-}$ antisymmetric stretching vibrations, and those at 1007 and 985 cm^{-1} to the ν_1 $(SO_4)^{2-}$ symmetric stretching vibrations. Infrared band at 924 cm^{-1} is connected with the ν_3 $(UO_2)^{2+}$ antisymmetric stretching vibrations and that at 855 cm^{-1} to the

Tab. 6 Atom coordinates and displacement parameters for the crystal structure of rietveldite from the Giveaway-Simplot mine

	x/a	*y/b*	*z/c*	U_{eq}	U^{11}	U^{22}	U^{33}	U^{23}	U^{13}	U^{12}
U	0.25237(2)	0.61331(4)	0.77723(17)	0.01437(12)	0.01737(16)	0.01493(19)	0.0108(2)	0.0009(3)	–0.00054(16)	–0.00116(10)
Fe1	0.5	0.8254(3)	0.43215(19)	0.0288(6)	0.0166(10)	0.0381(15)	0.0318(16)	0.0028(13)	0	0
Fe2	0	0.8361(3)	0.46263(17)	0.0241(5)	0.0173(8)	0.0295(12)	0.0253(13)	–0.0003(10)	0	0
S1	0.27336(19)	0.2620(4)	0.5849(3)	0.0189(5)	0.0218(9)	0.0200(14)	0.0149(13)	–0.0002(12)	–0.0009(12)	0.0011(11)
S2	0.25309(13)	0.7560(4)	0.4660(3)	0.0147(6)	0.0164(11)	0.0169(15)	0.0109(15)	–0.0015(12)	0.0013(7)	0.0006(8)
O1	0.1613(4)	0.2521(10)	0.5861(8)	0.0345(18)	0.025(3)	0.050(5)	0.028(4)	–0.006(4)	0.002(3)	–0.010(3)
O2	0.3231(6)	0.1180(8)	0.6324(8)	0.036(2)	0.044(5)	0.023(4)	0.040(5)	0.012(4)	–0.002(4)	0.012(3)
O3	0.3097(5)	0.4002(8)	0.6575(7)	0.035(2)	0.034(4)	0.030(5)	0.041(5)	–0.028(4)	–0.003(3)	0.004(3)
O4	0.3135(5)	0.2865(9)	0.4623(6)	0.0276(16)	0.031(3)	0.041(5)	0.011(3)	–0.002(3)	0.001(3)	–0.003(3)
O5	0.1628(6)	0.8593(10)	0.4608(8)	0.034(2)	0.017(3)	0.028(5)	0.058(6)	0.000(4)	0.005(3)	0.002(3)
O6	0.2321(7)	0.6007(13)	0.4103(15)	0.047(3)	0.060(6)	0.042(7)	0.041(8)	–0.008(5)	–0.004(5)	0.002(4)
O7	0.3397(5)	0.8370(10)	0.4071(7)	0.0308(19)	0.019(3)	0.044(5)	0.028(5)	0.021(4)	0.004(3)	–0.003(3)
O8	0.2838(5)	0.7235(9)	0.5895(7)	0.0296(16)	0.048(3)	0.029(4)	0.012(4)	0.008(3)	0.001(4)	0.008(4)
O9	0.3803(4)	0.6595(9)	0.8101(6)	0.0263(16)	0.023(3)	0.035(4)	0.021(4)	–0.007(3)	–0.002(3)	–0.006(3)
O10	0.1230(4)	0.5668(8)	0.7420(6)	0.0256(16)	0.021(3)	0.029(4)	0.027(4)	–0.008(3)	–0.006(2)	0.002(3)
OW1	0.2107(6)	0.9057(8)	0.7644(9)	0.0348(18)	0.056(4)	0.021(4)	0.028(5)	–0.004(4)	0.003(5)	–0.001(3)
OW2	0.5	0.8611(18)	0.6150(12)	0.045(4)	0.034(7)	0.087(12)	0.015(7)	–0.008(7)	0	0
OW3	0.5	0.7799(17)	0.2515(10)	0.045(4)	0.012(4)	0.112(11)	0.012(7)	–0.019(6)	0	0
OW4	0.5	0.5718(18)	0.4779(19)	0.066(5)	0.030(6)	0.038(8)	0.129(17)	0.017(10)	0	0
OW5	0.5	0.0873(18)	0.4182(17)	0.042(4)	0.021(5)	0.045(8)	0.061(10)	0.003(8)	0	0
OW6	0	0.8633(17)	0.6460(11)	0.040(4)	0.053(8)	0.061(10)	0.007(6)	0.007(6)	0	0
OW7	0	0.0852(16)	0.4459(17)	0.039(4)	0.020(5)	0.025(6)	0.072(12)	0.009(7)	0	0
OW8	0	0.7915(16)	0.2820(15)	0.048(3)	0.038(5)	0.082(10)	0.022(7)	–0.021(8)	0	0
OW9	0	0.5794(15)	0.4971(15)	0.040(3)	0.037(6)	0.029(7)	0.053(9)	0.000(7)	0	0

* Refined Fe2 site occupancy: 0.65(4) Fe, 0.35(4) Zn

Tab. 7 Selected bond distances (Å) for rietveldite from the Giveaway-Simplot mine

U–O9	1.742(6)	Fe1–OW3	2.076(11)	Fe2–OW8	2.074(17)
U–O10	1.766(5)	Fe1–OW2	2.087(14)	Fe2–OW7	2.081(13)
U–O6	2.338(13)	Fe1–O7 (×2)	2.099(6)	Fe2–OW6	2.084(13)
U–O8	2.346(8)	Fe1–OW4	2.172(15)	Fe2–O5 (×2)	2.118(7)
U–O3	2.350(7)	Fe1–OW5	2.184(15)	Fe2–OW9	2.170(13)
U–O4	2.407(7)	<Fe1–O>	2.120	<Fe2–O>	2.108
U–OW1	2.496(7)				
$<U1–O_{ap}>$	1.754	S1–O1	1.454(5)	S2–O5	1.453(8)
$<U1–O_{eq}>$	2.387	S1–O2	1.463(7)	S2–O6	1.463(12)
		S1–O3	1.489(7)	S2–O7	1.468(7)
		S1–O4	1.493(7)	S2–O8	1.475(9)
		<S1–O>	1.465	<S2–O>	1.475
Hydrogen bonds					
OW1–O2	2.732(11)	OW3–O1 (×2)	2.817(10)	OW7–O1	2.967(14)
OW1–O7	2.758(11)	OW5–O4	2.972(11)	OW8–O2 (×2)	2.945(14)
OW2–O9 (×2)	3.174(14)	OW6–O10	3.130(14)	OW9–O10 (×2)	3.194(17)

Note that hydrogen bonds to other H_2O groups are not listed

ν_1 $(UO_2)^{2+}$ symmetric stretching vibrations. Inferred approximate U–O bond lengths in uranyl are 1.73 and 1.76 Å, respectively (Bartlett and Cooney 1989). Weak band at 708 cm^{-1} may be related to libration mode of H_2O molecules. Bands at 655, 633 and 598 cm^{-1} are attributed to the triply degenerate ν_4 (δ) $(SO_4)^{2-}$ bending vibrations and ones at 512 and 466 cm^{-1} to the ν_2 (δ) $(SO_4)^{2-}$ doubly degenerate bending vibrations.

Approximate U–O bond lengths and hydrogen bond lengths inferred from observed ν_1 and ν_3 $(UO_2)^{2+}$ stretching vibrations and ν OH stretching vibrations of water molecules are in agreement with those inferred from X-ray structure analysis.

7. X-ray crystallography and structure determination

7.1. Powder diffraction

X-ray powder diffraction data (Tab. 3) were obtained from a hand-picked Jáchymov sample using a Bruker

Tab. 8 The bond-valence analysis for rietveldite from the Giveaway-Simplot mine

	U	Fe1	Fe2	S1	S2	hydrogen bonds	Σ
O1				1.58		0.18, 0.18, 0.14	2.07
O2				1.55		0.21, 0.14, 0.14	2.04
O3	0.56			1.44			2.00
O4	0.50			1.42		0.14	2.06
O5			$0.33^{\times 2\downarrow}$		1.59		1.92
O6	0.58				1.55		2.12
O7		$0.35^{\times 2\downarrow}$			1.52	0.20	2.08
O8	0.57				1.50		2.06
O9	1.81					0.10, 0.10	2.02
O10	1.73					0.11, 0.10, 0.10	2.05
OW1	0.42						
OW2		0.36					
OW3		0.37					
OW4		0.29					
OW5		0.28					
OW6			0.36				
OW7			0.37				
OW8			0.37				
OW9			0.29				
Σ	6.18	2.01	2.06	5.99	6.15		

Hydrogen bond contributions and bond-valence sums for OW sites are not included

* Fe2–O bond strengths based upon refined site occupancy; Fe^{2+}–O bond-valence parameters from Kanowitz and Palenik (1998); Zn^{2+}–O and S^{6+}–O from Brown and Altermatt (1985); U^{6+}–O from Burns et al. (1997); hydrogen-bond strengths based on O–O bond lengths from Ferraris and Ivaldi (1988)

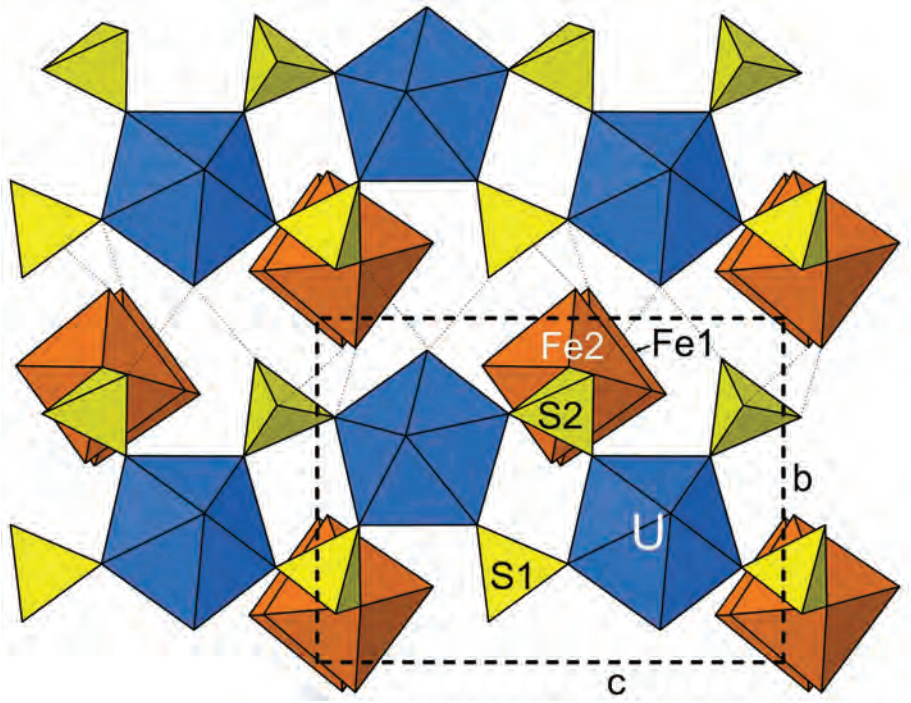

Fig. 10 The structure of rietveldite viewed down [100]. Interlayer hydrogen bonds are shown as faint dotted lines. The unit cell is outlined by dashed lines. Note the $[(UO_2)(SO_4)_2(H_2O)]$ chain along [010].

D8 Advance diffractometer equipped with a solid-state 1D LynxEye detector using CuK_α radiation (40 kV and 40 mA) and operating in Bragg-Brentano geometry (National Museum, Prague). Data were collected in the range 4–75° 2θ, with the step size of 0.01° and counting time of 30 s per step (total counting time was *c*. 3 days). Positions and intensities of diffractions were refined using a PearsonVII shape function in the program ZDS (Ondruš 1993). Unit-cell parameters were refined by least-squares with the program by Burnham (1962). Refined unit-cell parameters of rietveldite from Jáchymov obtained from powder data are: a = 12.9557(5), b = 8.3098(3), c = 11.2915(4) Å, with V = 1215.64(6) Å^3 and Z = 4.

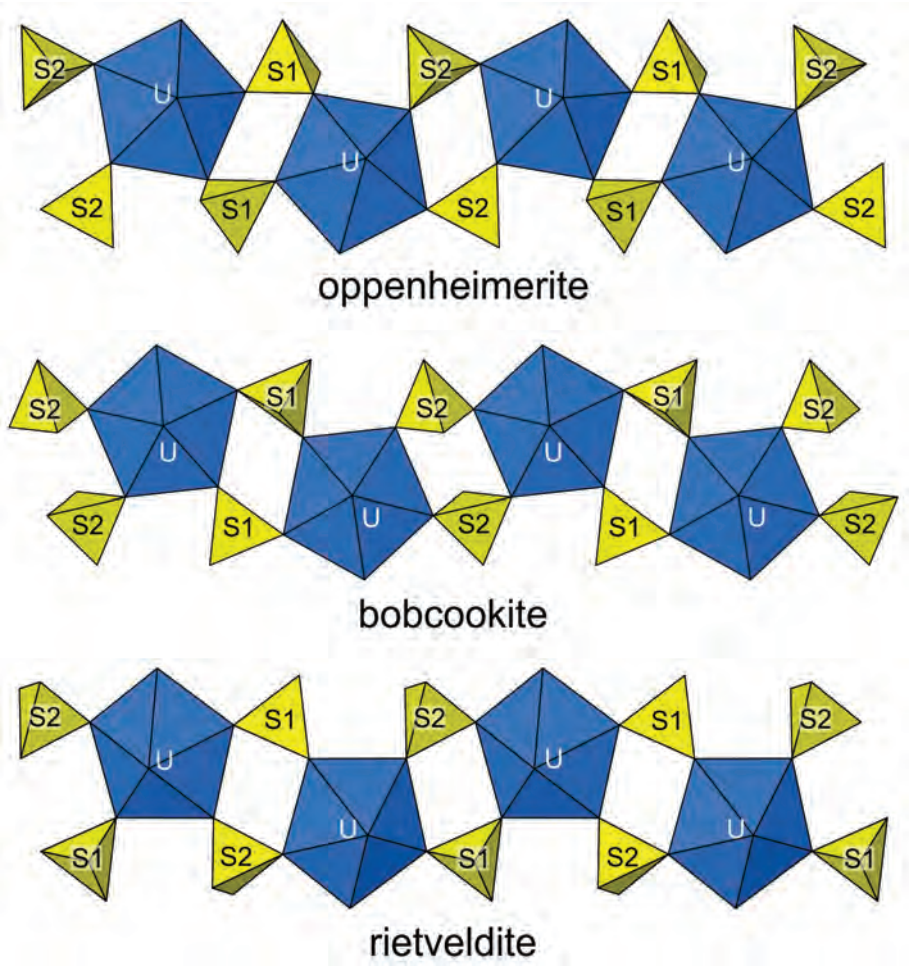

Fig. 11 The $[(UO_2)(SO_4)_2(H_2O)]^{2-}$ uranyl sulfate chains in the structures of oppenheimerite, bobcookite and rietveldite. Note the geometrical isomerism of the SO_4 groups.

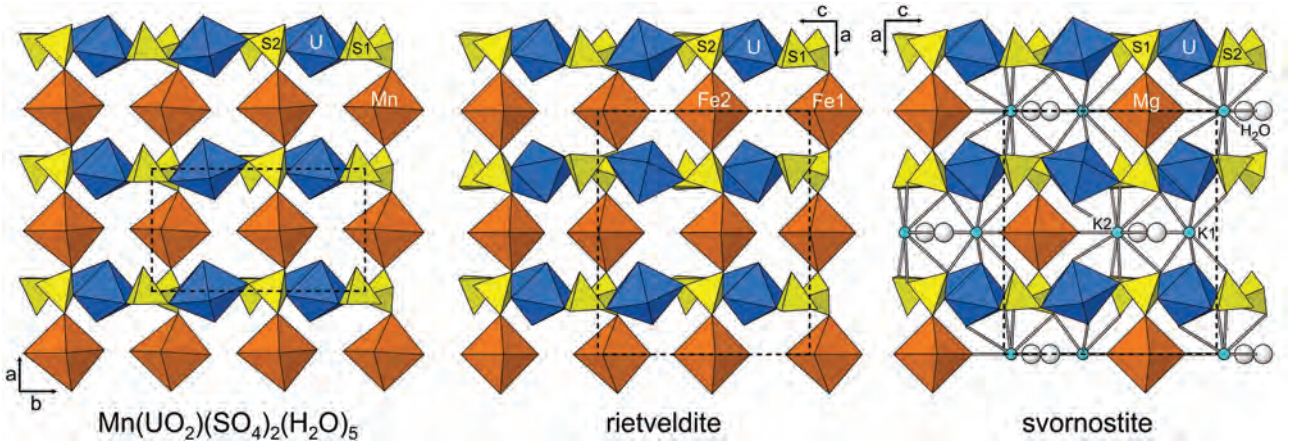

Fig. 12 The structures of synthetic $Mn(UO_2)(SO_4)_2(H_2O)_5$, rietveldite and svornostite. The unit cells are outlined by dashed lines. Note the identical geometries of the uranyl sulfate chains (viewed on-edge) and the polytypic relationship between $Mn(UO_2)(SO_4)_2(H_2O)_5$ and rietveldite.

7.2. Single-crystal X-ray diffraction and structure solution

A prismatic single crystal of rietveldite from Give-away-Simplot, with dimensions 0.18 × 0.09 × 0.005 mm^3, was selected under the microscope and diffraction data were collected using a Rigaku R-Axis Rapid II curved imaging plate microdiffractometer with monochromatized MoK_α radiation. According to diffraction data, rietveldite is orthorhombic with a = 12.9577(9), b = 8.3183(3), c = 11.2971(5) Å, with V = 1217.7(1) Å^3 and Z = 4 (Tab. 4). The Rigaku CrystalClear software package was used for processing the structure data, including the application of an empirical multi-scan absorption correction using ABSCOR (Higashi 2001).

The crystal structure of rietveldite was solved using SIR2011 (Burla et al. 2012). The software SHELXL-2013 (Sheldrick 2015) was employed for the refinement of the structure. The reflection conditions and statistics indicated orthorhombic primitive cell and the non-centrosymmetric space group $Pmn2_1$. The structure solution located all non-hydrogen atoms, which were refined with anisotropic displacement parameters. The Fe1 site refined to full occupancy by Fe and the Fe2 site refined to 0.65 Fe and 0.35 Zn. All other sites were assigned full occupancies. The H atoms locations could not be found in the difference Fourier maps. Data collection and refinement details are given in Tab. 5, atom coordinates and displacement parameters in Tab. 6, selected bond distances in Tab. 7, and results of a bond valence analysis in Tab. 8.

7.3. Description of the crystal structure

The U site in the structure of rietveldite is surrounded by seven O atoms forming a squat UO_7 pentagonal bipyramid. This is the most typical coordination for U^{6+} in solid state, particularly in uranyl sulfates, where the two short apical bonds of the bipyramid constitute the uranyl group, $(UO_2)^{2+}$. Four of the five equatorial O atoms of the UO_7 bipyramid participate in SO_4 tetrahedra; the other is an H_2O group. The linkages of pentagonal bipyramids and tetrahedra form an infinite $[(UO_2)(SO_4)_2(H_2O)]^{2-}$ chain along [001]. The chains

Tab. 9 Comparison of unit cell parameters for rietveldite and related compounds

	Rietveldite	Svornostite	Synthetic	Synthetic	Synthetic
Ideal formula	$Fe(UO_2)(SO_4)_2(H_2O)_5$	$K_2Mg(UO_2)_2(SO_4)_4(H_2O)_8$	$Fe(UO_2)(SO_4)_2(H_2O)_5$	$Mg(UO_2)(SO_4)_2(H_2O)_5$	$Mn(UO_2)(SO_4)_2(H_2O)_5$
Crystal system	orthorhombic	orthorhombic	orthorhombic	orthorhombic	monoclinic
Space group	$Pmn2_1$	$Pmn2_1$	*Pmmb*, $Pm2_1b$ or *P2mb*	*Pmmb*, $Pm2_1b$ or *P2mb*	$P2_1$
a (Å)	12.9577	12.7850	6.489	6.435	6.524
b (Å)	8.3183	8.2683	11.28	11.39	11.40
c (Å)	11.2971	11.2163	8.297	8.333	8.362
β (°)					90.78
V (Å^3)	1217.67	1185.68	607.3	610.8	621.85
Z	4	2	2	2	2
Reference	*This work*	Plášil et al. (2015)	Serezhkin and Serezhkina (1978)	Serezhkin and Serezhkina (1978); Soares Rocha (1960)	Serezhkin and Serezhkina (1978); Tabachenko et al. (1979)

* Note that rietveldite and svornostite cells have a parameters that are approximately double those of the synthetics; also the b and c axes are interchanged

are linked in the [100] direction by $Fe1O_6$ and $Fe2O_6$ octahedra, which share vertices with SO_4 tetrahedra. A heteropolyhedral sheet parallel to {010} is thereby formed. Adjacent sheets are linked by hydrogen bonding and Fe–O bonds (Fig. 10).

7.3. Structural relationships

The $[(UO_2)(SO_4)_2(H_2O)]^{2-}$ chain in the structure of rietveldite was also found in the structures of bobcookite, $Na(H_2O)_2Al(H_2O)_6[(UO_2)_2(SO_4)_4(H_2O)_2]\cdot 8H_2O$ (Kampf et al. 2015a), oppenheimerite, $Na_2(H_2O)_2[(UO_2)(SO_4)_2(H_2O)]$ (Kampf et al. 2015b), svornostite, $K_2Mg[(UO_2)(SO_4)_2]_2\cdot 8H_2O$ (Plášil et al. 2015), synthetic $K_2[(UO_2)(SO_4)_2(H_2O)](H_2O)$ (Ling et al. 2010) and synthetic $Mn(UO_2)(SO_4)_2(H_2O)_5$ (Tabachenko et al. 1979). These chains in oppenheimerite, bobcookite and rietveldite, compared in Fig. 11, are geometrical isomers, while the chains in rietveldite, svornostite and synthetic $Mn(UO_2)(SO_4)_2(H_2O)_5$ are virtually identical.

The structure of rietveldite is very closely related to that of synthetic $Mn(UO_2)(SO_4)_2(H_2O)_5$ and, presumably, to those of the other synthetic phases of general formula $M(UO_2)(SO_4)_2(H_2O)_5$, in which M = Mg, Mn, Fe, Co, Ni, Cu, Zn or Cd (*cf.*, Soares Rocha 1960; Serezhkin and Serezhkina 1978). The structures of rietveldite and $Mn(UO_2)(SO_4)_2(H_2O)_5$, compared in Fig. 12, are seen to be polytypes. Rietveldite has doubled the *a* cell parameter of $Mn(UO_2)(SO_4)_2(H_2O)_5$ and other synthetic $M(UO_2)(SO_4)_2(H_2O)_5$ phases (Tab. 9). Rietveldite and svornostite have the same space group and very similar cell parameters. Their structures, also compared in Fig. 12, are almost equivalent except that one of the octahedral sites (Fe1) and two H_2O sites (OW2 and OW3) present in the rietveldite structure are missing in the svornostite structure. These sites are replaced, although not in the same positions, by two K sites. Note that the powder diffraction patterns of rietveldite, svornostite and synthetic $Mn(UO_2)(SO_4)_2(H_2O)_5$ are almost identical.

Acknowledgements. We thank B. Ullrich (TU Bergakademie, Freiberg) for providing us SEM images. The current text benefited from the constructive comments of Oleg Siidra and Stuart Mills. František Laufek is thanked for editorial handling of the manuscript. This research was financially supported by the John Jago Trelawney Endowment to the Mineral Sciences Department of the Natural History Museum of Los Angeles County, by the institutional research plan AV010100521 of the Institute of Physics ASCR, v.v.i. and by the long-term project DKRVO 2017-01 of the Ministry of Culture of the Czech Republic (National Museum 000232782) to JS and JČ. Part of the analytical work was done using instrumentation at the ASTRA lab established within the Operation program Prague Competitiveness project CZ.2.16/3.1.00/24510.

Electronic supplementary material. Supplementary crystallographic data for this paper are available online at the Journal web site (*http://dx.doi.org/10.3190/jgeosci.236*).

References

Bartlett JR, Cooney RP (1989) On the determination of uranium–oxygen bond lengths in dioxouranium(VI) compounds by Raman spectroscopy. J Mol Struct 193: 295–300

Brown ID, Altermatt D (1985) Bond-valence parameters obtained from a systematic analysis of the inorganic crystal structure database. Acta Crystallogr B41: 244–248

Brugger J, Meisser N, Burns PC (2003) Contribution to the mineralogy of acid drainage of uranium minerals: marecottite and the zippeite-group. Amer Miner 88: 676–685

Burla MC, Caliandro R, Camalli M, Carrozzini B, Cascarano GL, Giacovazzo C, Mallamo M, Mazzone A, Polidori G, Spagna R (2012) SIR2011: a new package for crystal structure determination and refinement. J Appl Crystallogr 45: 357–361

Burnham CW (1962) Lattice constant refinement. Carnegie Institute Washington Yearbook 61: 132–135

Burns PC, Ewing RC, Hawthorne FC (1997) The crystal chemistry of hexavalent uranium: polyhedron geometries, bond-valence parameters, and polymerization of polyhedra. Canad Mineral 35: 1551–1570

Chenoweth WL (1993) The Geology and Production History of the Uranium Deposits in the White Canyon Mining District, San Juan County, Utah. Utah Geological Survey Miscellaneous Publications 93–3: pp 1–26

Čejka J (1999) Infrared spectroscopy and thermal analysis of the uranyl minerals. In: Burns PC, Finch RJ (eds) Uranium: Mineralogy, Geochemistry and the Environment. Mineralogical Society of America and Geochemical Society Reviews in Mineralogy and Geochemistry 38, Washington, pp 521–622

Fernandes HM, Veiga LHS, Franklin MR, Prado VCS, Taddei JF (1995) Environmental impact assessment of uranium mining and milling facilities; a study case at the Poços de Caldas uranium mining and milling site, Brazil. In: Allan RJ, Salomons W (eds) Heavy Metal Aspects of Mining Pollution and Its Remediation. J Geochem Explor 52: 161–173

Ferraris G, Ivaldi G (1988) Bond valence vs. bond length in O···O hydrogen bonds. Acta Crystallogr B44: 341–344

Finch RJ, Murakami T (1999) Systematics and paragenesis of uranium minerals. In: Burns PC, Finch RJ (eds) Uranium: Mineralogy, Geochemistry and the Environment.

Mineralogical Society of America and Geochemical Society Reviews in Mineralogy and Geochemistry 38, Washington, pp 91–179

Higashi T (2001) ABSCOR. Rigaku Corporation, Tokyo

Hloušek J, Plášil J, Sejkora J, Škácha P (2014) News and new minerals from Jáchymov, Czech Republic (2003–2014). Bull mineral-petrolog odd Nár Muz (Praha) 22: 155–181 (in Czech)

Kampf AR, Plášil J, Kasatkin AV, Marty J (2015a) Bobcookite, $NaAl(UO_2)_2(SO_4)_4(H_2O)_{18}$, and wetherillite, $Na_2Mg(UO_2)_2(SO_4)_4 \cdot 18H_2O$, two new uranyl sulfate minerals from the Blue Lizard mine, San Juan County, Utah, USA. Mineral Mag 79: 695–714

Kampf AR, Plášil J, Kasatkin AV, Marty J, Čejka J (2015b) Fermiite, $Na_4(UO_2)(SO_4)_3 \cdot 3H_2O$, and oppenheimerite, $Na_2(UO_2)(SO_4)_2 \cdot 3H_2O$, two new uranyl sulfate minerals from the Blue Lizard mine, San Juan County, Utah, USA. Mineral Mag 79: 1123–1142

Kampf AR, Kasatkin AV, Čejka J, Marty J (2015c) Plášilite, $Na(UO_2)(SO_4)(OH) \cdot 2H_2O$, a new uranyl sulfate mineral from the Blue Lizard mine, San Juan County, Utah, USA. J Geosci 60: 1–10

Kampf AR, Plášil J, Kasatkin, AV, Marty J, Čejka J, Lapčák L (2017) Shumwayite, $[(UO_2)(SO_4)(H_2O)_2]_2 \cdot H_2O$, a new uranyl sulfate mineral from Red Canyon, San Juan County, Utah, USA. Mineral Mag 81: 273–285

Kanowitz, Palenik (1998) Bond valence sums in coordination chemistry using oxidation-state-independent R_0 values. A simple method for calculating the oxidation state of iron in Fe−O complexes. Inorg Chem 37: 2086–2088

Krivovichev SV, Plášil J (2013) Mineralogy and crystallography of uranium. In: Burns PC, Sigmon GE (eds) Uranium: From Cradle to Grave. Mineralogical Association of Canada Short Courses 43: pp 15–119

Libowitzky E (1999) Correlation of O–H stretching frequencies and O–H···O hydrogen bond lengths in minerals. Monatsh Chem 130: 1047–1059

Ling J, Sigmon GE, Ward M, Roback N, Burns PC (2010) Syntheses, structures, and IR spectroscopic characterization of new uranyl sulfate/selenate 1D-chain, 2D-sheet and 3D framework. Z Kristallogr 225: 230–239

Loopstra BO, Rietveld HM (1969) The structure of some alkaline-earth metal uranates. Acta Crystallogr B25: 787–791

Mandarino JA (1976) The Gladstone-Dale relationship – Part 1: derivation of new constants. Canad Mineral 14: 498–502

Ondruš P (1993) ZDS – a computer program for analysis of X-ray powder diffraction patterns. Materials Science Forum, EPDIC-2, Enchede, 133–136, 297–300

Ondruš P, Veselovský F, Gabašová A, Hloušek J, Šrein V, Vavřín I, Skála R, Sejkora J, Drábek M (2003) Primary minerals of the Jáchymov ore district. J Czech Geol Soc 48: 19–147

Plášil J (2014) Oxidation–hydration weathering of uraninite: the current state-of-knowledge. J Geosci 59: 99–114

Plášil J, Sejkora J, Škoda R, Škácha P (2014) The recent weathering of uraninite from the Červená vein, Jáchymov (Czech Republic): a fingerprint of the primary mineralization geochemistry onto the alteration association. J Geosci 59: 223–253

Plášil J, Hloušek J, Kasatkin AV, Novák M, Čejka J, Lapčák L (2015) Svornostite, $K_2Mg[(UO_2)(SO_4)_2]_2 \cdot 8H_2O$, a new uranyl sulfate mineral from Jáchymov, Czech Republic. J Geosci 60: 113–121

Pouchou JL, Pichoir F (1985) "PAP" (φρZ) procedure for improved quantitative microanalysis. In: Armstrong JT (ed) Microbeam Analysis. San Francisco Press, pp 104–106

Reichel W, Schauer M (2006) Das Döhlener Becken bei Dresden. Bergbau in Sachsen, No. 12. Sächsisches Landesamt für Umwelt und Geologie, Dresden, pp 1–380 (in German)

Rietveld HM (1966) The crystal structure of some alkaline earth metal uranates of the type M_3UO_6. Acta Crystallogr 20: 508–513.

Rietveld HM (1967) Line profiles of neutron powder-diffraction peaks for structure refinement. Acta Crystallogr 22: 151–152

Rietveld HM (1969) A profile refinement method for nuclear and magnetic structures. J Appl Crystallogr 2: 65–71

Serezhkin VN, Serezhkina LB (1978) X-ray diffraction study of double uranyl sulphates $M(UO_2)(SO_4) \cdot 5H_2O$. Russ J Inorg Chem 23: 414–416

Serezhkin VN, Serezhkina LB (1982) On some properties of disulfatouranylate hydrates of divalent metals. Zh Neorg Khim 27: 424–430 (in Russian)

Serezhkina LB, Grigoryev AN, Serezhkin VN, Tabachenko VV (1979) Investigation of vibrational spectra of sulfatouranylate pentahydrates of divalent metals. Zh Neorg Khim 24: 1631–1634 (in Russian)

Sheldrick GM (2015) Crystal structure refinement with SHELX. Acta Crystallogr C71: 3–8

Soares Rocha N (1960) Synthesis and X-ray data of magnesium uranyl sulphate: $MgUO_2(SO_4)_2 \cdot nH_2O$. An Acad Brasil Ciênc 32: 341–343

Tabachenko VV, Serezhkin VI, Serezhkina LB, Kovba LM (1979) Crystal structure of manganese sulfatouranylate $MnUO_2(SO_4)_2(H_2O)_5$. Koord Khim 5: 1563–1568 (in Russian)

Thalheim K, Reichel W, Witzke T (1991) Die Minerale des Döhlener Beckens. Schriften des Staatlichen Museums für Mineralogie und Geologie zu Dresden 3: pp 1–131 (in German)

Young RA (1993) Introduction to the Rietveld method. In: Young RA (ed) The Rietveld Method. IUCr Book Series, Oxford University Press, Oxford, pp 1–39

Yvon K, Jeitschko W, Parthé E (1977) Lazy Pulverix, a computer program for calculation X-ray and neutron diffraction powder patterns. J Appl Crystallogr 10: 73–74